MICROMACHINED THERMOGENERATOR FOR HIGH-TEMPERATURE APPLICATIONS

Azat Ibragimov[1*], Walter Lang[1]
[1] Institute for Microsensors, -actuators and -systems (IMSAS), University of Bremen, Bremen, Germany
*Presenting Author: aibragimov@imsas.uni-bremen.de

Abstract: A thermally and mechanically stable Seebeck-effect based thermogenerator is described, which is conceived primarily for high-temperature applications such as automotive thermogenerators working with exhaust temperatures of 700°C or more. The device realization is based on novel technological process, which implements amorphous borosilicate glass as substrate material and monocrystalline silicon as main voltage generating material. The effective 77% usage of the chip surface and low total resistivity were achieved. The thermogenerator was tested up to 730°C, thus already nearing the softening point of borosilicate glass. The maximal power output of 515 µW is achieved at $\Delta T \approx 600$°C by the load impedance of 47 kOhm, thus confirming the low contact resistivity value.

Keywords: Seebeck, silicon, borosilicate glass, high-temperature

INTRODUCTION

The rapid progress of the later years in the field of distributed sensor systems accelerates also the development of accompanying "energy-harvesting"-devices. The application of such systems would be useful for the structure-health-monitoring in the harsh environment, where the risks of malfunctioning overweight the costs of additional equipment. The corresponding "energy-harvesters" should be able not only to withstand such harsh conditions but to take an advantage of them.

Many of those critical harsh-environment-applications are associated with high temperature gradient (e.g. industrial ovens, exhaust pipes or oil pans of combustion engines), making especially worthwhile the implementation of Seebeck-effect based thermogenerators (TG). Such applications require thermal and, because of the corresponding thermomechanical stress, mechanical stability of the TG. Even more, since the power output of a TG is proportional to the square of the generated potential difference, the effective usage of the thermal flow is needed. The later means, that the voltage generating material should have high Seebeck-coefficient on the whole temperature range between the heat source and the cold sink.

Due to high temperature gradient involved and respectively high potentially possible power output, the same approach could be applied to common energy gaining applications such as automotive thermoelectric generator working with exhaust temperatures of 700°C or more.

The design, fabrication and characterization of the TG, which meets these requirements, is the subject of the paper.

DESIGN

The TG consists principal of a substrate with 32 thermocouples (TC) on its surface. The TC have the semiconductor part, which plays the major role in generating the thermopower and the interconnecting metal part, whose Seebeck coefficient is negligible in compare with those of the semiconductor chosen. The enlarged semiconductor ends of the fringe TCs are also covered with a metal layer and used as bond pads. The whole TG is 4x6 mm^2 a size with the working area of 3.3x4 mm^2.

Substrate

In order to minimize the thermal conductivity of the TG, the 500-µm-thick borosilicate glass (BSG) was chosen as substrate material. What is more, such amorphous substrate does not have crystal planes, which often are the propagation direction of arising defects, and thus provides better stability against mechanical stress, which oft arises in the high-temperature environment. The softening point of BSG is 810 °C. Since all other materials, used in the TG, are more thermally stable, this temperature sets the upper limit to the TG's working range.

Thermocouples

Figure 1 depicts the TC's schematic (the substrate is not shown) with semiconductor and metal parts of TC. The later are placed in the grooves etched in the former and they are everywhere but on the contact pads, separated from each other by the 400-nm thick silicon oxide layer. This layer was also removed around the grooves, thus providing place for the bonding of the BSG-substrate. The cross section of the semiconductor parts is 77 µm x 40 µm and the interval between them - 23µm.

Figure 2 depicts the TG from the structured side and as it is seen through the transparent BSG-substrate. The proposed design intends the metal conductors to be placed not between the semiconductor parts of the TG but beneath them. Therefore the effective usage of the chip's working surface was achieved (voltage generating parts cover 77% of it).

The practically identical coefficient of thermal expansion of silicon and BSG prevents the arising of significant inner thermomechanical stress in the TG. Additionally the wavy form of TCs should reduce the probability of their breaking under the outer mechanical stress, exerted on the chip by surrounding materials. At high temperatures such outer stress will be also at least partially absorbed by the BSG-substrate, as it becomes softer.

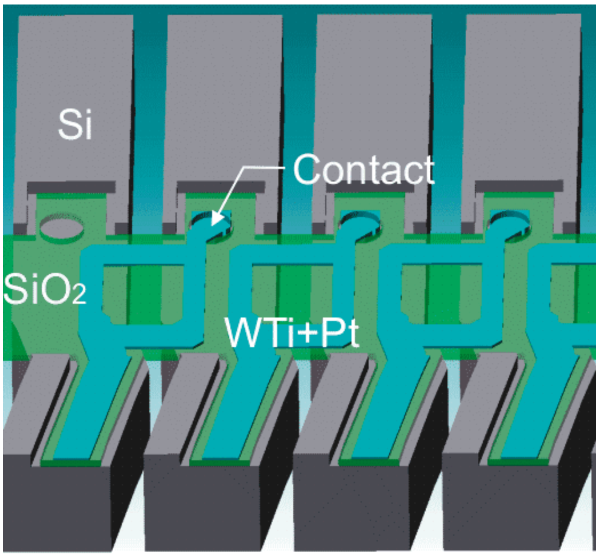

Fig. 1: Schematic of thermocouples.

For the TC's semiconductor part the n-type monocrystalline silicon was chosen. Popular thermoelectrical materials, which have high Seebeck-coefficient at standard conditions, deteriorate at higher temperatures. For instance, the homogeneity limit of Bi_2Te_3 is 586°C [1], more than that: the minimal 0.2%-variation of the Te-concentration in the initial mixture causes its fall to 460°C [2]. Or the solid–solid phase transition point of HgCdTe is 410°C [3]. This makes plausible the use of silicon for high-temperature applications. The choice of the n-type dopant was dictated by the fact, that the Seebeck coefficient of the p-type silicon changes its sign as the semiconductor approximates to the intrinsic area, thus negatively affecting the whole generated potential difference. The dopant concentration of $3*10^{17}\left[cm^{-3}\right]$ was chosen.

In order to provide good ohmic contact between the silicon and metal interconnections the aluminum is often used [4], [5]. But this layer is not enough thermally stable, therefore in this work the TC's metal parts are made primarily of Pt (main conduction layer – 180 nm), although this material shows poor adhesion to the silicon and silicon oxide especially under thermomechanical stress. In order to solve the problem an additional adherent layer was added. Aiming to the high-temperature working region, the stable $W_{0.1}Ti_{0.9}$ -alloy (40 nm) for the later was chosen, which however causes high-ohmic contacts at room temperature, thus limiting the TG's working range from below.

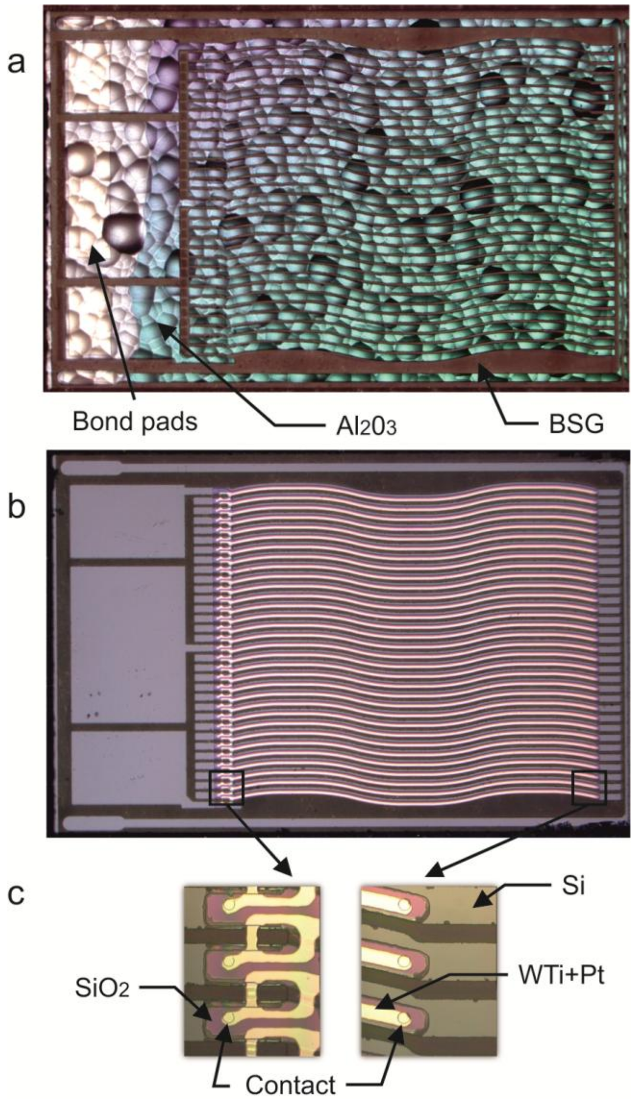

Fig. 2: Thermogenerator: (a) view from the structured side, (b) view through the transparent BSG-substrate, (c) blow-ups of the contact windows between Si and WTi+Pt.

FABRICATION TECHNIQUE

The fabrication steps are shown in figure 3. The four represented stadiums include six photolithography steps. In sequence:

- a) grooves definition, creating windows for the contact between silicon and metal, definition of the TC's metal parts
- b) exposure of the wafer surface around the grooves and removing the exposed part of the silicon oxide layer for the following anodic bonding
- c) from the back side – definition of the metallic bond pads, wafer thinning, definition of the TC's silicon parts and subsequently their DRIE-etching
- d) the profiling of the Al_2O_3-isolation layer does not require high resolution photolithography and is made by the means of the screen printing. This step opens the bond pads

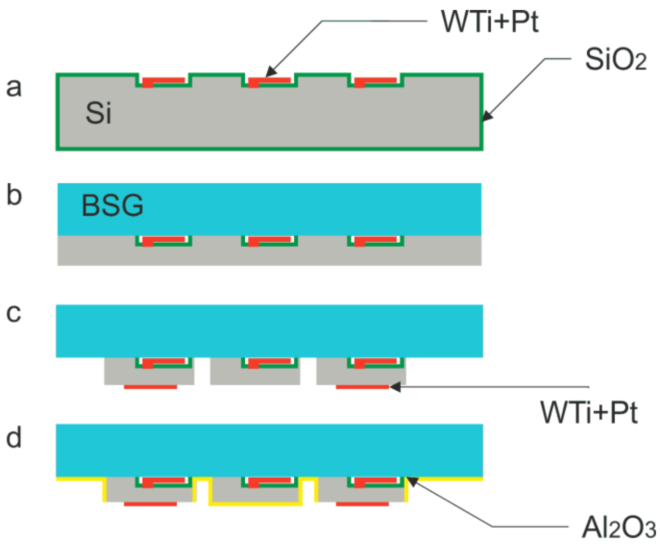

Fig. 3: Fabrication of the TG: (a) oxidized Si-wafer with metal parts of TCs, placed in grooves with contact windows at ends, (b) partial SiO2 removal, anodic bonding and wafer thinning, (c) fabrication of contact pads and DRIE, (d) deposition of the isolation layer.

Since the grooves are only 1µm deep, all critical photolithography steps are made on the practically flat surface. Thus was avoided the limitation on the thickness of the silicon parts, caused by necessity of the photolithography on deep relief structures. This together with the above mentioned effectiveness of the surface usage allows the significant reduction of TG's inner resistivity (19 kOhm at room temperature).

CHARACTERIZATION AND DISCUSSION

Figure 4 depicts the total resistivity, which is the sum of the inner and contact resistivities, of two TG-chips from two different wafers versus the environment temperature.

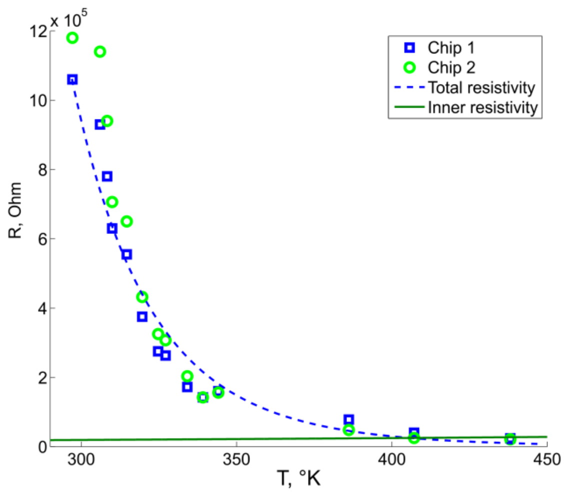

Fig. 4: Experimental temperature dependence of total resistivity of two TGs in comparison with theoretical values of the inner resistivity.

The solid line represents the TG's calculated inner resistivity, based on the dopant concentration in silicon. Due to high dopant concentration, the inner resistivity rises with temperature, showing in this temperature range the metal-like behavior. Despite the low inner resistivity the total impedance is compromised at room temperature by the resistivity of contacts between the WTi-adherent layer and silicon. Nevertheless the contact resistivity drops rapidly with the temperature rising, thus ensuring the TG's effective usage in elevated temperature environment. Such exponential contact characteristics are often associated with some kind of p-n-junction structures. Their exact nature will be addressed separately in future works. At 165°C the contact resistivity practically equals zero and the total TG's impedance is determined by its inner resistivity, thus allowing to approach maximal theoretically possible power output with the semiconductor given. This temperature determines the lower border of the TG's working range.

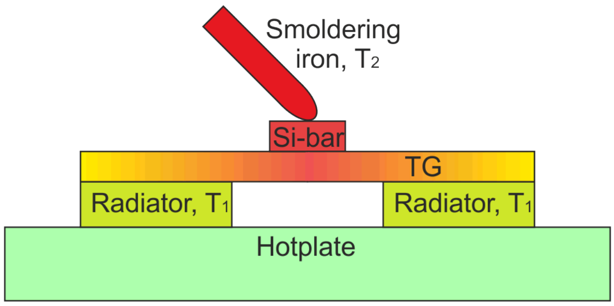

Fig. 5: Schematic of the experimental set-up.

The schematic of the experimental set-up is depicted in figure 5. The chip composed of two mirrored TGs was fixed on the radiator with a hole in its middle. The bond pads and the adjacent row of contact pads lay on the radiator. The small thermal difference between them and the radiator is ensured by the layer of a thermal paste, applied under the chip on the radiator surface. The radiator itself is placed on the regulated hotplate. The apposite rows of contact pads in the middle of the double chip are placed over the hole in the radiator. From above they are covered by a silicon bar, which ensures homogenous temperature distribution among them. The hot tip of a regulated electric smoldering iron is applied to the silicon bar, thus creating the temperature gradient in the TCs. The direct measurement of the temperature distribution on the TG's surface is difficult to obtain with the given experimental set-up, therefore the temperatures of the smoldering iron's tip and of the radiator were taken as the temperatures of the TC's hot and cold ends respectively. These temperatures were measured by a contact thermocouple.

During the TG's tests the smoldering iron's tip was heated up to 730°C thus already nearing the softening point of BSG. The radiator's temperature was kept around 120°C, thus ensuring low contact resistivity on the TC's cold ends.

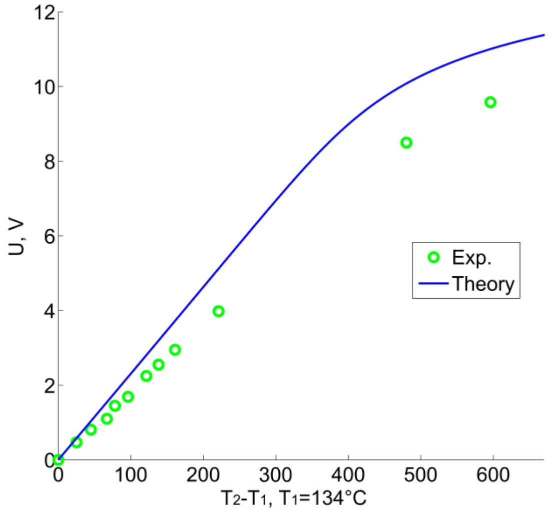

Fig. 6: Experimental points for open loop voltage versus the temperature difference in comparison with theoretical dependence.

Figure 6 presents the open loop voltage versus the temperature difference and shows that TG's thermoelectrical properties do not deteriorate at high temperatures. The difference between the theoretical curve and the experimental points is caused by the discrepancy between the real temperatures of the contact pads and their approximation, given by the temperatures of the iron's tip and the radiator.

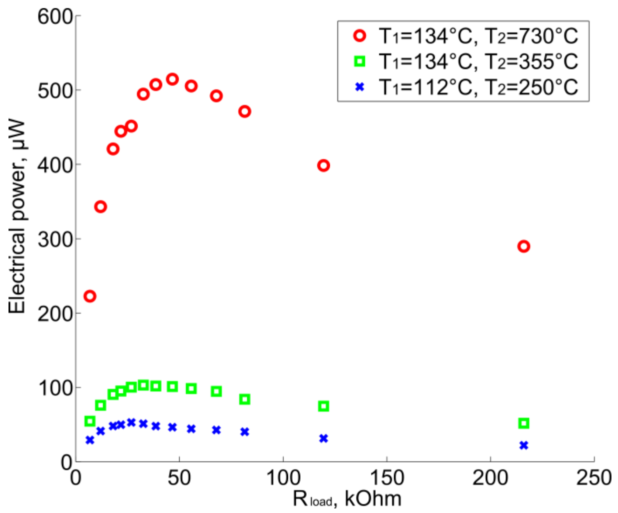

Fig. 7: Experimental points for power output versus consumer resistance at different temperature differences.

Figure 7 depicts the power output versus consumer resistance for three different temperature distributions. The output power is maximal when the TG is balanced, so the peeks of these curves give us the TG's total resistivity (27, 33 and 47 kOhm respectively), thus confirming low contact resistivity value. The maximum power output of 515 µW was archived at $\Delta T \approx 600$°C.

CONCLUSION

The novel technological process allows the fabrication of thermally and mechanically stable MEMS-structures, which was demonstrated on the example of a Seebeck-effect-based TG. Thought its working range is limited from below by high contact resistivity of WTi-Si-connections, the TG can be effectively applied in high-temperature environment. It was tested up to 730°C and did not lose its functionality. Considerable power output of 515µW was achieved.

Possible application fields of the developed TG can also include its embedding in metal, glass or ceramic components during their manufacturing (e.g. casting process), what will be the subject of further researches. The possibility of other MEMS-implementation of the introduced technology will be considered.

ACKNOWLEDGEMENT

The work has been sponsored by the Deutsche Forschungsgemeinschaft (German Research Foundation) within the Project "Integration thermoelektrischer Generatoren in metallische Gussteile" ("Integration of thermoelectric generators in metal castings").

REFERENCES

[1] T. C. Harman, B. Paris, S. E. Miller, H. L. Goering, "Preparation and some physical properties of Bi_2Te_3, Sb_2Te_3, and As_2Te_3", *Journal of Physics and Chemistry of Solids*, **Volume 2**, Issue 3, 1957, Pages 181-190

[2] R. F. Brebrick, "Homogeneity ranges and Te_2-pressure along the three-phase curves for Bi_2Te_3(c) and a 55-58 at.% Te, peritectic phase", *Journal of Physics and Chemistry of Solids*, **Volume 30**, Issue 3, March 1969, Pages 719-731

[3] J. Zhao, X. Li, H. Liu, R. Jiang, Z. Liu, Z. Hu, H. Gong, J. Fang, "Damage threshold of HgCdTe induced by continuous-wave CO2 laser," *Applied Physics Letters*, **vol.74**, no.8, p.1081, Feb 1999

[4] H. Glosch, M. Ashauer, U. Pfeiffer, W. Lang, "A thermoelectric converter for energy supply", *Sensors and Actuators A*: Physical, **Volume 74**, Issues 1-3, 20 April 1999, Pages 246-250

[5] N. Kockmann, T. Huesgen, P. Woias, "Micro-structured in-plane thermoelectric generators with optimized heat path," *Solid-State Sensors, Actuators and Microsystems Conference*, 2007. TRANSDUCERS 2007. International , 2007